Hybrid PCM-steam thermal energy storage for industrial processes

Niknam, Pouriya H; Sciacovelli, Adriano

DOI:
10.1016/j.apenergy.2022.120358

Document Version
Publisher's PDF, also known as Version of record

Citation for published version (Harvard):
Niknam, PH & Sciacovelli, A 2023, 'Hybrid PCM-steam thermal energy storage for industrial processes: Link between thermal phenomena and techno-economic performance through dynamic modelling', *Applied Energy*, vol. 331, 120358. https://doi.org/10.1016/j.apenergy.2022.120358

Applied Energy 331 (2023) 120358

Contents lists available at ScienceDirect

Applied Energy

journal homepage: www.elsevier.com/locate/apenergy

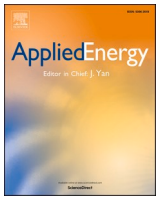

Hybrid PCM-steam thermal energy storage for industrial processes – Link between thermal phenomena and techno-economic performance through dynamic modelling

Pouriya H Niknam, Adriano Sciacovelli *

School of Chemical Engineering, Birmingham Centre for Energy Storage, University of Birmingham, UK

HIGHLIGHTS

- A dynamic model for HyTES is implemented to estimate the performance and optimise the design.
- The surpassing efficiency of HyTES arises from PCM latent heat and the superior performance of the steam accumulator in the hybrid system.
- HyTES stores up to 45% more energy than a conventional steam accumulator.
- The incorporation of HyTES leads to 5% reductions in CAPEX and stream generation cost.
- The dominant design parameter for HyTES are the PCM latent heat and the charging time.

ARTICLE INFO

Keywords:
Thermal energy storage
Hybridisation
Phase change materials (PCM)
Steam accumulator
Industry
Efficiency

ABSTRACT

This study aims to assess the performance and economics of novel hybrid thermal energy storage (HyTES) for industrial applications, linking performance to thermal phenomena occurring within the system. The storage hybridisation concept is based on coupling latent heat storage modules containing high-temperature Phase Change Materials (PCMs) with a fast-response steam accumulator. Such hybrid storage, where heat is stored in both forms of steam and latent heat of PCMs, has the potential to capture excess heat produced by the steam generator of any industrial processes, which can then be used at peak times. HyTES performance is dynamically modelled during charging, idle, and discharging stages. The results show that the HyTES provides 14% extra energy storage capacity than the existing steam accumulator within an identical total volume. Furthermore, the study provides technical analysis of HyTES, and thorough comparison between configurations with different PCM volumes, PCM types and charging times. This is essential to ultimately quantify the whole range of benefit of hybrid energy storage. The sensitivity analysis reveals that Incorporating the HyTES significantly improves energy capacity, and the degree of improvement is mainly affected by the charge duration, approximately 15% after 1 h, and 45% after 4 h of charging. Furthermore, it is shown how the PCM properties affect the performance of HyTES. Finally, the CAPEX and O&M cost of the entire system are assessed in different scenarios and found to be 5% less when HyTES replaces the conventional SA.

1. Introduction

Over the past decade, there has been a dramatic rise in energy prices, and emission regulations have become more stringent. Also, world leaders have pledged at COP26 (UN Climate Change Conference) to cut emission levels by 50–60 % by 2050, as part of efforts to tackle the climate crisis. In order to meet this objective, global emissions needed to fall by 52–58 GtCO2e/yr by 2030, and by 20–24 GtCO2e/yr by 2050 [1]. On the other hand, the industry is responsible for nearly a quarter of the total emissions, and it is expected that it delivers a proportionate share of emissions cuts [2]. The policies for the industry in the global net-zero strategy include the support for improving their energy resource and energy efficiency [3]. Therefore, energy efficiency enhancement has ranked among the top priorities for industries. Within such context, several waste heat recovery technologies have been developed to support energy management and facilitate decarbonisation. Thermal energy storage systems (TES), as one of the emerging waste heat recovery

* Corresponding author.
E-mail address: a.sciacovelli@bham.ac.uk (A. Sciacovelli).

https://doi.org/10.1016/j.apenergy.2022.120358
Received 17 May 2022; Received in revised form 30 September 2022; Accepted 14 November 2022
Available online 29 November 2022

Nomenclature

Symbols

B	Boiler
CO_2e	CO_2 equivalent
H	Specific enthalpy [kJ/kg]
kt	kilotonne
L	Liquid
LH	Latent heat [kJ/kg]
M	Total mass [kg]
m	mass flow [kg/s]
R_2	radius of HyTES [m]
R_1	Radius of SA [m]
S	Solid
T	Temperature [K]
t	time [*sec*]
x	PCM liquid fraction
Q	Convective Heat flux

Superscripts and subscripts

I	*index*
L	Liquid
out	Outlet
cond	Condensation
evap	Evaporation
in	Inlet
pc	phase change
sat	Saturation
V	Vapour
τ	time constant [s]
ϕ	Energy flow

technologies, have the potential to enhance energy resilience by storing the heat for later use, which leads to promoting energy utilisation efficiency aligned with the decarbonisation goals.

TES is classified into three major types based on the principle of operation: latent heat thermal energy storage (LHTES), sensible thermal energy storage (STES) and thermochemical energy storage (TCS), which have been extensively reviewed for example in [45]. Sensible TES and LHTES are mature technologies or near to market to drive deep decarbonisation of industry. Instead, TCS is in the development stage, but it is not moving nearly fast enough to accelerate on some fronts [6]. They have distinctive features in terms of storage timeframe, capacity, response time, and temperature range.

More recently, a number of studies have emerged on TES solutions with hybrid configuration seeking solutions for either upgrading material characteristics or improving the storage system efficiency. The key concept behind hybridisation is the combination either individual TES principles, materials or systems within a single and integrated TES system with the purpose of ultimately deliver performance or functions that the isolated TES subsystem would not be able to achieve [7]. With the context and aim of the present work, the focus is on hybrid thermal energy storage (Hy-TES) combining sensible TES and LHTES. The advanced development and adoption stage of such two TES technologies provides clear routes for hybridisation, while the TCS advancement still requires overcoming fundamental development challenges. Hence hybridisation options involving TCS technologies remain currently to a great extent out of reach.

Proposed hybridisation of Sensible TES and LHTES has so far been conceived to take advantage of the key distinctive features of these two types of TES. On one side, the cost effectiveness and rapid energy charge/discharge of sensible TES, particularly when the storage medium is in liquid form. On the other hand, the higher energy storage density, stable operating conditions and a wide range of candidate PCMs for energy storage at different temperature levels.

An exemplar case of Hybridisation of sensible TES and LHTES has been put forward by Zauner et al. [8]. They hybridised industrial-scale shell-and-tubes TES in which latent heat was provided by high-density polyethylene placed inside the tubes, while sensible storage of heat was provided by thermal oil on the shell side. The experimental and numerical results demonstrated that such hybridisation gave significant versatility to the TES system, both from design and operational points of view. High power storage could be achieved with small diameter tubes, even for low PCM conductivity. Similarly, designs with fewer tubes increased the share of sensible TES, leading to quicker charge/discharge. Conversely, more packed designs (either larger tubes or higher number of tubes) are favourable where energy storage density and constant operating temperatures are essential for the end-use application.

Hybridisation between sensible TES with solid storage medium and LHTES has instead been proven to be successful when optimisation of energy storage density and specific costs needs to be concurrently taken in consideration [9]. An exemple investigation of such hybridisation strategy has been carried out by Liu et al. [9], who considered a variety of PCMs storage media and graphite for combined latent-sensible storage of thermal energy at high temperature (~500 – 750 °C) at MWh scale. Overall, the proposed HyTES was estimated to achieve a cost reduction between 7 and 14 % compared with a PCM-based cascade storage while largely delivering comparable operating conditions.

Relevant to the work presented in this paper are the recent developments of hybrid TES system encompassing steam accumulation. Recently, Dusek et al. [9 10] investigated the joint operation of steam accumulation and PCM in a hybrid configuration in which a thin layer of PCM was integrated with the outer shell of the steam storage vessel. Such hybrid system has the potential to store thermal energy form of both steam and heat, which are commonly necessary for industrial processes. The increase in energy storage capacity of the hybrid system compared to the conventional steam TES storage was reported to be 29 %. Similarly, Pernsteiner et al. [11] implemented a numerical model of the hybrid system, and their estimation showed about 25 % increase in the energy capacity. However, the authors raised the issue of the excessive computational cost required for the CFD simulation. Moreover, the dynamic behaviour of steam storage during the charging/discharging cycle is less discussed, and the CFD simulation was limited to the PCM. Kasper et al. [12] also showed how PCM element orientation, the fraction of aluminium and fin spacing significantly affect the thermal behaviour of the PCM within the hybrid steam accumulation-LHTES systems. However, the simulation was limited to a single PCM element, and thus the influence of steam storage was included exclusively through equivalent thermal boundary conditions. Finally, work from Hoffman et al. [13], which extended the study of Dusek et al., addressed the optimum design for retrofitting steam storage systems with PCM containers leading to additional energy storage capacity from 10 % to 40 %. However, their economic assessment was based on the CAPEX only, and no running costs were taken into account. In contrast, there are other studies like the one by Venettacci et al. (2022) [14], where the coupling of PCM-based TES with gas-fired boiler is experimentally explored and the results covers the operating cost reduction by 21.4 % and in fuel saving by 18.4 %; However the case study developed for supplying domestic hot water.

Overall, it has therefore emerged that, from the technical point of view, research on the hybrid PCM-steam storage systems to date has focused on providing evidence on the feasibility of PCM incorporation into conventional steam storage vessels. Works have been mostly focused on modelling of the PCM part of the steam accumulator, while

comprehensive technical assessments are to a good extent currently missing due to a general lack of a complete modelling framework for estimating unsteady behaviour under realistic conditions emerging from integrating the storage system into end-user processes.

Furthermore, from an economic standpoint, published studies on HyTES combining steam accumulation and LHTES have so far marginally assessed costs in a holistic manner, often only capturing a fraction of the overall costs involved. Such limitation of existing studies is particularly relevant for applications of HyTES in the industrial context – which is the focus of the present work. In most industries, operational costs are rolling parameters often of the same order of magnitude as the investment cost [15,16]. Hence, neglecting O&M costs in evaluating HyTES technology may lead to underestimating the economic viability. Nonetheless, it remains of paramount importance that holistic cost analysis is paired with accurate technical analysis. Hence the aim and scope of the present work, which addresses such need by means of a first-of-a-kind comprehensive techno-economic investigation of HyTES consisting of steam accumulation and LHTES with PCMs for medium temperature applications in an industrial setting.

Specifically, the overarching aim and scope of this work is to quantitatively answer a set of integrated techno-economic questions to a) fundamentally understand the enhanced technical operability, technical efficiency, and eventual technical limitations provided hybrid steam accumulation - LHTES system and b) to thoroughly assess the costs, value and benefits unlocked by the investigated HyTES for its applicability and integration within a specific industrial process with thermal energy demand in the form of steam and heat. Additionally, and complementarily, the present work also proposes a high-fidelity and computationally effective modelling approach that allow to thoroughly simulate the dynamic behaviour of the HyTES system in fine detail such that the technical and economic characteristics of the problem are fully and comprehensively captured.

1.1. Novelty and originality of this work

The work here focuses on a superior and holistic study of the techno-economic performance of HyTES consisting of a fully coupled steam accumulator and LHTES using PCMs for storage of thermal energy in the range of 150–250 °C. In particular, the work contributes to advancing the understanding of thermo-fluid dynamic behaviour of the system and how this is intimately intertwined with its technical performance and economic viability. Compared with prior contributions reviewed in Section 1, the present paper takes an alternative route and poses particular attention to how the phase change phenomenon within the PCMs, and the dynamic behaviour of steam accumulation/discharge processes link to overall system performance. Further, in addition, the work thoroughly establishes the causal correlations and sensitivities between the fundamental thermal phenomena occurring within the hybrid system, its performance and the overall costs of the system itself, both at the design stage as well as during operation. Ultimately, methods and results presented here advance the understanding of the benefits and trade-offs of HyTES solutions, which have been so far largely overlooked. In doing so, the present work contributes to advancing the technology closer to a technically and economically viable implementation in real-life conditions.

2. Hybrid thermal energy storage – System description and its application context

Steam is one of the most widely used and highly effective mediums for industrial heating. It is an integral part of various industries, including food, beverage, textile, chemical, medical, power, and manufacturing [17]. Steam accumulators (SA) are a common solution to separate the boiler output from sudden load variations and enhance the continuity and reliability of the steam supply.

Fig. 1 shows different pathways considered in this work in order to meet steam demand in an industrial process. Key to the present work is the energy storage (buffer component) section. Here, two alternatives have been considered: i) traditional steam accumulation by means of SA or ii) Hybrid thermal energy storage (HyTES), which consists of combined steam accumulation and thermal energy storage, the latter by means of phase change materials (PCMs). The rationale for this choice lies in the increase in energy storage capacity as well as steam accumulation capacity enabled by the use of PCMs, as fully detailed in the Results Section of this work.

Fig. 2 illustrates more technical details of HyTES investigated in this work. The concept was originally proposed by Dusek et al. [1318]. However, as outlined in Section 1.1, the work in this manuscript significantly differs from existing literature by thoroughly establishing the causal correlations and sensitivities between the fundamental thermal phenomena occurring within the hybrid system, its performance and the techno-economic benefits. The PCM layer covers the external shell of the SA and thus exchanges heat with steam/water contained within the SA. Thus, thermal energy is stored in two media: water/steam

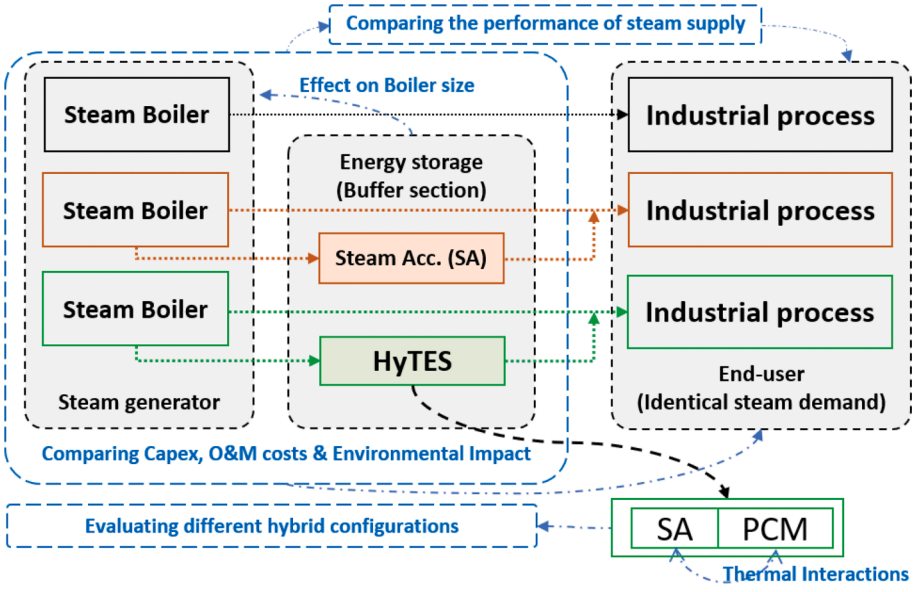

Fig. 1. Outline of scenarios responding to steam demand of industrial process.

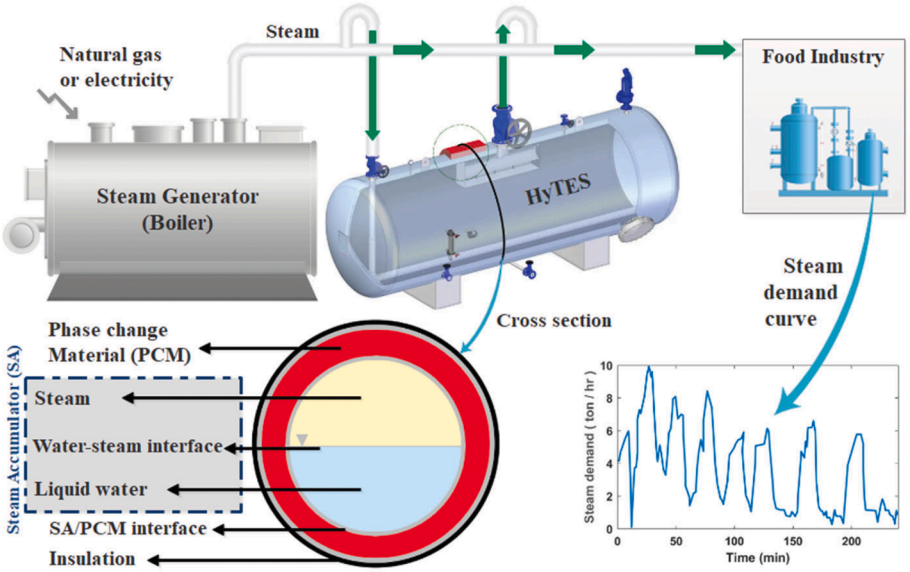

Fig. 2. The incorporation of HyTES in the industrial steam supply chain.

and PCMs. The interplay between these two key parts of the system is therefore expected to alter the overall charging/discharging performance as well as storage capacity, as fully detailed in the subsequent sections of this manuscript. Finally, Fig. 2 also illustrates how the HyTES could be integrated in an industrial process. Specifically to this work, integration with food processing industry. The case study has been selected based on two criteria: first, it should be from the industrial sector with high steam demand, i.e. chemical, steel and food industries. The availability of steam demand profile was the second reason why we chose the current case, which is related to the food industry. The steam demand is taken from the literature [19].

3. Methodology

The methodological framework adopted in this work consists in a technical analysis and an economic assessment. On the technical side, the HyTES dynamic behaviour is simulated to investigate the performance of the hybrid configuration. The comparison between steam storage and HyTES was performed to reveal the potential improvement in energy capacity. Meanwhile, the sensitivity analysis identified the influential parameters. The derived energy enhancement index is used to calculate HyTES cost and the consequent financial impact on the industrial end-user.

3.1. Technical assessment basics

3.1.1. Steam storage subsection

The total convective heat exchange which takes place between the fluid and the environment, Q, is given by the sum of the heat transfer rates between phases (water and steam) and the environment:

$$Q = Q_L + Q_V \tag{1}$$

The phase change and the consequent heat and mass transfer are determined by vaporisation and condensation processes. The energy flow associated with either evaporation or condensation when the specific enthalpy is greater or less than the saturation specific enthalpy is calculated by Equation (2):

$$\phi = M(H - H_{sat})/\tau \tag{2}$$

where M and H, and τ are the total liquid or vapour mass and specific enthalpy and time constant, and either the evaporation or condensation mass flow rate is assessed by Eq. (3) [20]:

$$m = \phi/H_{sat} \tag{3}$$

The primary model determines phase change in the water-steam equilibrium state; however, the total volume is constant. Steam flow and phase change rates in the accumulator are governed by the mass balance equations for the liquid and vapour which is defined by Equation (4) [20]:

$$\frac{dm_{L/V}}{dt} = \dot{m}_{in} - \dot{m}_{out} + \dot{m}_{cond/evap} \tag{4}$$

in which $\dot{m}_{in}$ and $\dot{m}_{out}$ are the inlet and outlet mass flow rates.

The water can be heated or cooled depending on the heat transfer between the tank and the environment. Equation (5) and equation (6) are the energy balance in the liquid and vapour, respectively.

$$M_L\frac{du_L}{dt} + \frac{dM_L}{dt}u_L = \phi_{L,in} - \phi_{L,out} + \phi_{cond} - \phi_{evap} + Q_L \tag{5}$$

$$M_V\frac{du_V}{dt} + \frac{dM_V}{dt}u_V = \phi_{V,in} - \phi_{V,out} - \phi_{cond} + \phi_{evap} + Q_V \tag{6}$$

in which ϕ_{in}, ϕ_{out}, ϕ_{cond}, ϕ_{evap} are inlet, outlet, condensation and evaporation energy flow rates.

3.1.2. PCM subsection

PCM is a type of energy storage material which is based on a phase-changing process, typically a solid to liquid and vice versa. Hence, the primary storage principle of PCM is latent heat. However, the sensible heat, defined as thermal mass, serves as an additional heat storage mechanism. The sensible heat is simply defined as Equation (7) to store the energy in the form of internal energy:

$$Q_i = C_{p,pcm}m_i\frac{dT_i}{dt} \tag{7}$$

One hundred nodes are employed in radial direction to precisely locate the phase boundary within the PCM layer. This number of elements is chosen so that doubling them results in less than a 1 % change in the interface location. Individual cell thickness and corresponding cell mass (m_i) are calculated based on the total thickness of the PCM in cylindrical coordination:

The thickness of elements is identical. The temperature and the phase state are determined by the energy balance., The energy (Q_i) absorbed by or released from each node during the system operation

derived by Equation (8) [21]:

$$Q_i = \begin{cases} m_i C_p (T_{pc} - T_i) & T < T_{pc} (x_i = 0) \\ m_i LH & T = T_{pc} (0 < x_i < 1) \\ m_i C_p (T_i - T_{pc}) & T < T_{pc} (x_i = 1) \end{cases} \quad (8)$$

T_{pc} and LH are phase-change temperature and latent heat of ith element of PCM block. The element temperature remains unchanged in the phase change process until the entire volume changes into either liquid or solid. Meanwhile, as described by Equation (9), the corresponding phase fraction is assessed using the heat and the latent heat. The phase fraction is bounded within 0 and 1, referring to the entirely liquid and solid states.

$$x_i = max(min\left(\left[x_{S,0} + \int_{t0}^{t} \frac{Q(t)}{m_i.LH} dt\right], 1\right), 0) \quad (9)$$

In order to model the entire PCM, the governing equations must be solved for all elements which are located in a row and linked together by conductive heat transfer. The key input for each element is the energy flow, while other parameters are set according to the material property and operating conditions.

3.1.3. HyTES model

The HyTES consists of a cylindrical SA surrounded by PCM. A one-dimensional transient numerical approach is developed to model the charging/discharging cycle of the HyTES. The steam storage and PCM models are considered as HyTES subsystems which are interconnected by a conductive thermal link. The SA subsystem is responsible for the mass balance and VLE calculations, while the PCM subsystem provides the progression of phase front during the charge/discharge process and its effects on the PCM temperature. The heat flux with time is then calculated with an energy balance accounting for conductive heat transfer between SA and PCM, as shown in equation (10).

$$Q_L + Q_v + Q_{PCM,interface} = 0 \quad (10)$$

The control of SA is done by charging and discharging control valves. A 2-hour time window is considered for the simulation, and the valve commands are shown in Fig. 3, which start with upstream valve opening, followed by idle time and downstream valve opening.

An algebraic system of equations is solved in each time step in order to advance the solution. It is solved by ODE113 solver in MATLAB Simscape, and key parameters are tracked through time during the simulation, including the heat flux, mass flow rates, SA liquid level, PCM phase front and the temperature of all elements. The numerical assumptions are listed in Table 1, including fixed values and ranges in which ranges are the design space for the sensitivity analysis to explore the behaviour of HyTES. These ranges are defined based on the property of commercial high-temperature salt PCMs, including PlusICE® H190 to PlusICE® H220 [22], with the latent heat of 100 to 170 kJ/kg. Those PCMs with phase temperatures within the range of the minimum and maximum steam saturation temperatures of the SA are suitable for the HyTES. Based on the literature, the characteristics of these PCMs are similar to solar salt and mixtures of nitrate salts [23].

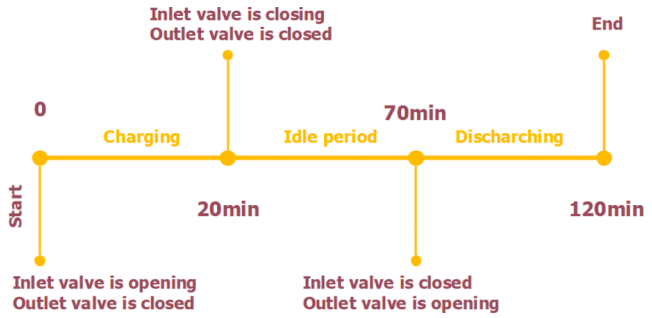

Fig. 3. Timeline of operation and valve actions.

Table 1
Technical assumptions.

Section	Parameter	Value or range	Reference
SA	Charging steam pressure [bara]	26	
	Charging steam Temperature [°C]	Saturated	
	Charging/ discharging Steam vapour quality	1	
	Discharging steam pressure [bara]	20	
	Initial water level	60 %	
	Diameter [m]	2	
	Length [m]	8.4	
	Steam/water heat transfer coefficient [W/(m^2 K)]	4700	[18]
Wall	Thermal conductivity [W/(m.K)]	46.5	
	Thickness [mm]	20	
	Density [kg/(m^3)]	7800	
	Specific heat capacity [J/(kg.K)]	490	
PCM	Thickness [mm]	20–70	
	Latent heat [kJ/(kg)]	100–170	[22]
	Specific heat capacity [J/(kg.K)]	1500–1600	[22]
	Density [kg/(m^3)]	200–2300	
	Phase change temperature [°C]	191–220	
	Thermal conductivity [W/(m.K)]	0.52	[22]
Insulation	Thermal conductivity [W/(m.K)]	0.035	

3.1.4. Validation

Before proceeding to discuss the results, it is essential to validate our individual implementations for both steam storage and PCM technologies. In order to validate the nonequilibrium model of the steam accumulator, the simulation is adapted to the condition of the case study of Stevanovic et al. [24]. The pressure is demonstrated in Fig. 4, which is compared with reference in the charging for a steam storage with 11 m of length and 2.9 m of diameter. The storage operates between 55 bar and 34 bar, and the relaxation time for the phase change process is 85 s.

Moreover, the PCM model is adapted for the experiments done by Siyabi et al. [25], which is a single-pass shell and tube reactor. A heat transfer fluid (HTF) flows inside a stainless tube, and the commercial-grade PCM is in the shell. Fig. 5 clearly demonstrates that The PCM phase gradually changes from solid to liquid while the energy transfers from the HTF to the PCM. The phase change process is associated with the forced convection at the inner radius and the natural convection with the ambient air at the reactor surface.

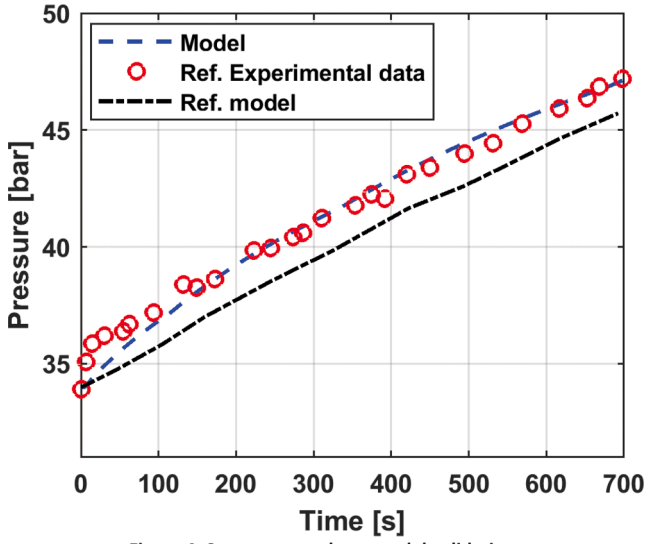

Fig. 4. Steam accumulator model validation.

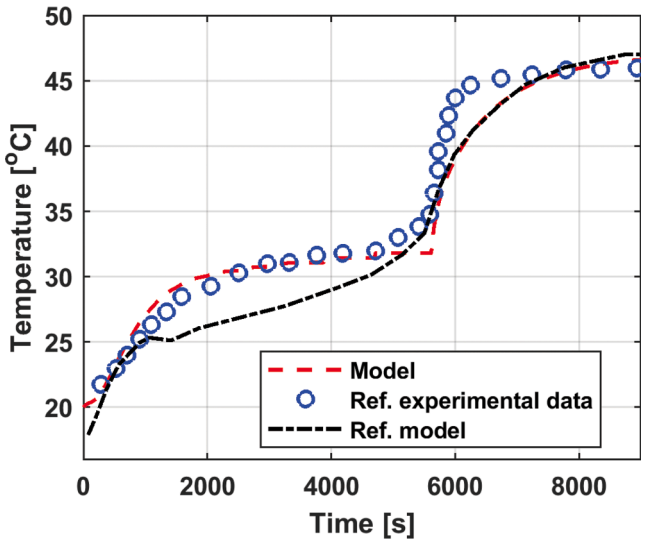

Fig. 5. PCM model validation.

4. Results

4.1. Dynamic performance of hybrid thermal energy storage under complete charge–discharge cycles

This section reports and discusses the dynamic behaviour of the HyTES system under investigation. As part of the overall aims of the paper, the results initially detail how the hybrid nature of the system leads to enhanced technical operability and efficiency compared to traditional TES systems. Therefore, the full charge–discharge cycle is considered to better isolate the thermal behaviour of the individual parts of the Hy-TES and the mutual interdependencies. Fig. 6 details the nominal full cycle under which the fundamental behaviour of the Hy-TES is investigated. The charging process is initiated through the opening of the steam inlet valve, which leads to steam flowing into the accumulator, as well as thermal energy being stored within the PCMs (as further detailed in this section). The Hy-TES system is considered as fully discharged at the beginning of the cycle. Following an idle period, the full discharge process is considered until the complete discharged state is reached. According to the references [26], this timescale is typical for the SA operation in industry.

4.1.1. Dynamic behaviour of steam accumulation and release during full charge–discharge cycle of the HyTES system

Since steam is the main heat carrier for transferring thermal energy between the HyTES system and the external end-user of thermal energy (See Section 2), it is essential to fully understand how steam flow rate and steam/water level of the HyTES dynamically vary during the charge and discharge processes. To this purpose, Fig. 7 shows the time evolution of the steam flow rate of the HyTES system under the storage cycle presented in Fig. 6. Positive values of flow rates correspond to the charging phase, during which steam enters and accumulate within the HyTES system. Conversely, negative flow rates reported in Fig. 7 correspond to HyTES discharging. During this stage, the steam previously accumulated is extracted from the HyTES system and delivered to the end-user.

Results in Fig. 7 clearly demonstrate that the steam flow rate is intrinsically unsteady during the operation of the system, with an initial spike, both during charge and discharge, in which a progressive reduction of flow until full charge or discharge is reached. Such dynamic behaviour is directly linked to the time evolution of pressure during the whole charge/discharge cycle. The steam flow rate is directly proportional to the pressure differential between feed line pressure and SA pressure. This differential is at its maximum at the very beginning of the charging process, leading to a higher value of steam mass flow rate. However, as the process is carried out, the pressure differential diminishes, as does, accordingly, the mass flow rate. Analogously, during discharge, larger steam flow rates are attained at the start of the process when the pressure inside the system is highest.

Fig. 7 also compares the HyTES steam flow rate with the one for a conventional steam accumulator, also known as Ruth steam accumulator or simply steam accumulator (SA). The comparison is carried out considering that the HyTES and the SA have the same volume available for the accumulation of steam, as well as identical inlet/outlet conditions during the charge and discharge processes. Fig. 7 highlights that during charging, the steam flow rate is slightly higher for the HyTES compared to the SA. Conversely, the mass flow rate for HyTES is found to be lower than for SA during discharging.

Fig. 8 complements the results of Fig. 7 and reports how the time evolution of the pressure and liquid level in the steam storage are intimately tied to the steam flow rate. The liquid level is proportional to the amount of steam that is condensed during charging or vapourised during discharging. On the other hand, both condensation and evaporation depend on the water-steam equilibrium state, which is pressure-dependent. The accumulation of steam during the charging causes an increase in pressure, as well as the saturation temperature, and therefore

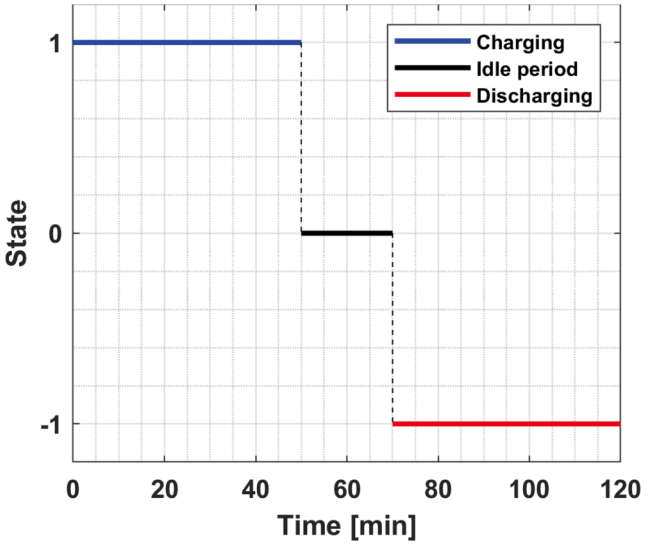

Fig. 6. Full duty cycle of the HyTES.

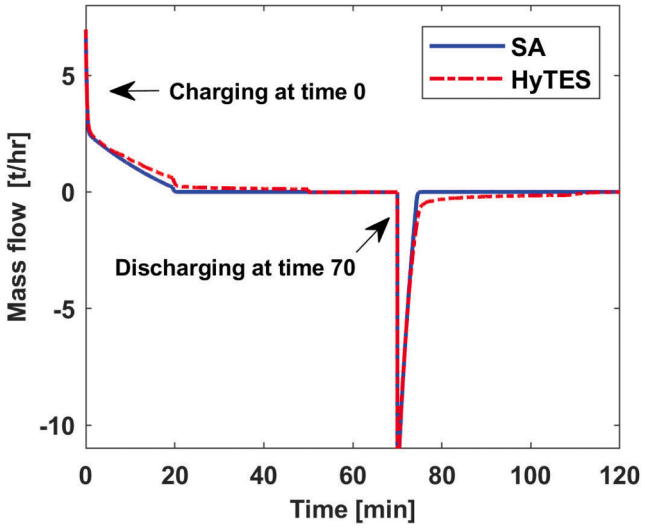

Fig. 7. Charging/discharging flow rate for both SA and HyTES.

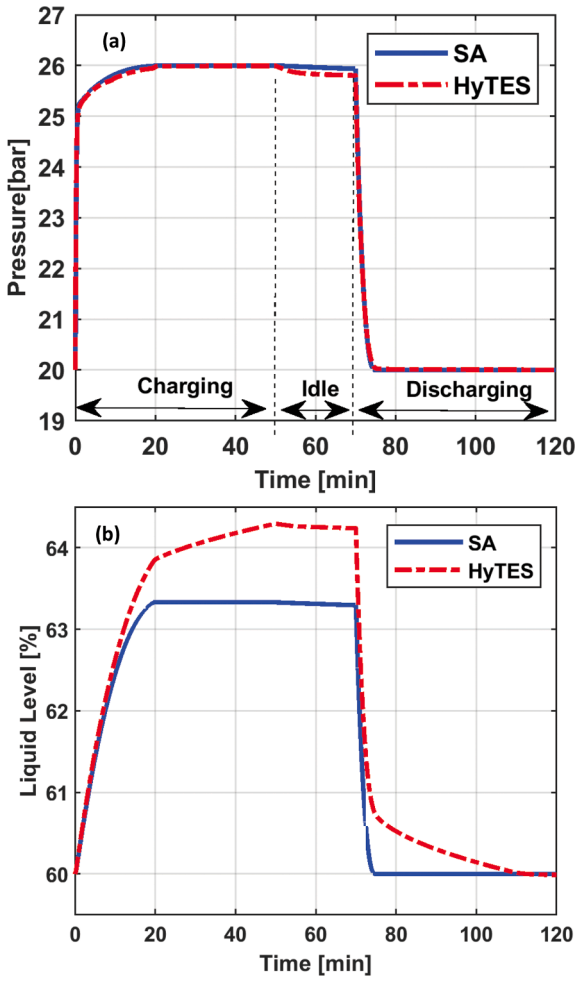

Fig. 8. Pressure (a) and liquid level (b) in steam storage for the conventional and hybrid designs.

the steam is partially condensed until the equilibrium is reached again. Fig. 8a also shows that during the charging process, the pressurisation of the system is nearly instantaneous; conversely, the condensation occurring during discharge is a relatively slow process. Both liquid level and the pressure remain unchanged until the discharging is initiated; thus, steam is released. In this step, the storage is depressurised from idle stage pressure to outlet pressure (~10 bar) in less than 5 min, while the liquid level decline takes place in a longer time frame to reach its final level.

Fig. 8 also compares the liquid level and the pressure in HyTES with those in SA. The heat transfer between the water/steam mixture and the PCM occurs at a slow rate; this can be appreciated in Fig. 8b from $t = 20$ min onwards. Here, the liquid level within the HyTES keeps increasing compared to the SA. This is due to the continuous transfer of heat from the steam/water to the PCM, which in turn leads to further condensation and hence an increase in the liquid level. Also, differently from the SA, HyTES shows a minor pressure drop during the idle period. Furthermore, the pressure is slightly lower than that in the SA (Fig. 8a) when the heat is continuously exchanged from steam to the PCM due to the temperature difference, and the difference is significant at the end of the idle period. The water level is also higher in the HyTES due to the thermal interaction between PCM and steam. The PCM intensifies the condensation rate by absorbing the heat from the steam during the charging, and therefore the liquid level in HyTES is found higher than that in SA. The thermal response of the PCM also alters the rate at which water level varies during discharging. In particular, the water level within the HyTES diminishes at a slower rate in comparison to a traditional SA. This can be immediately understood by recalling that during discharge, the thermal energy stored in the PCM is released and transferred to steam/water, thus diminishing the rate at which steam condenses.

4.1.2. *Dynamic behaviour of PCM during full charge–discharge cycle of the HyTES system*

This section illustrates and discusses the behaviour of the latent thermal energy storage (LHTES) subsystem integrated into the overall HyTES system. In the present study, two approaches are taken to precisely identify the effect of PCM in HyTES. The first analysis is based on fixed total volume, and PCMs occupy a part of the vessel. The second analysis is more aligned with the retrofitting of the existing steam accumulators, and the model is based on a vessel with a fixed dimension and various amounts of PCM. Therefore, the overall volume depends on the amount of embedded PCM. During charging and discharging of the whole HyTES system thermal energy is exchanged between the steam within the steam accumulator and the external compartments containing the PCMs. Fig. 9 illustrates the outline of the system with the moving interface of liquid and solid phases in PCM. Consequently, melting of the PCMs and thus storage of thermal energy occurs during the steam accumulation process within the HyTES system. Conversely, when steam is retrieved from the HyTES system, and thus energy is progressively extracted from the system, the PCMs solidify and release the heat previously stored. Hence the radial position of the PCM melting front dynamically changes.

The time evolution of such interface position is reported in Fig. 10. It shows the charging and discharging processes that take place during the duty cycle previously presented (Fig. 6). Approximately 5 min after the start of the charging process (steam injected in the accumulator), the PCM begins to melt, and the melting front progressively advances from the inner wall until reaching the outer wall (maximum radius). Similarly, during discharge (steam released from the accumulator), the solidification process starts at t = 70 min from the inner wall and progresses until all of the PCM solidifies.

The time evolution of HyTES system temperature is reported in Fig. 11. The graph illustrates the temperature for water/steam as well as the PCM at different radial positions. As expected, the PCM located closer to the inner wall (i.e. at smaller radial coordinates) exchanges heat with the water/steam during the initial stages of the charging/discharging process. Consequently, the PCM temperature at such locations raises/decreases during the early stages of the charge/discharge

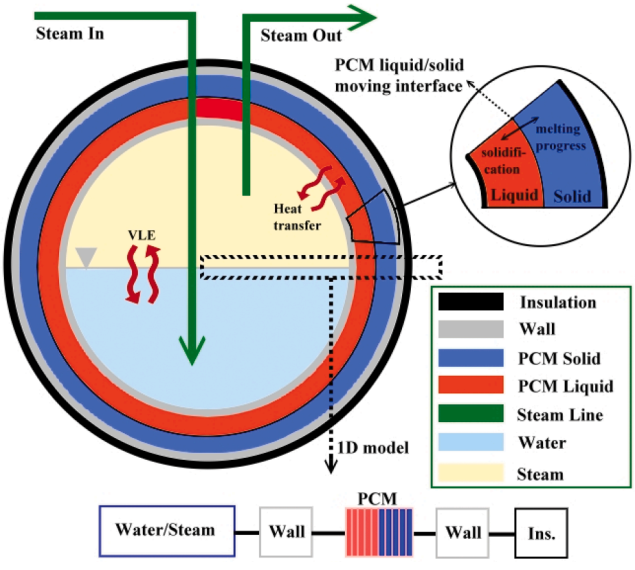

Fig. 9. Identification of the PCM melting front location.

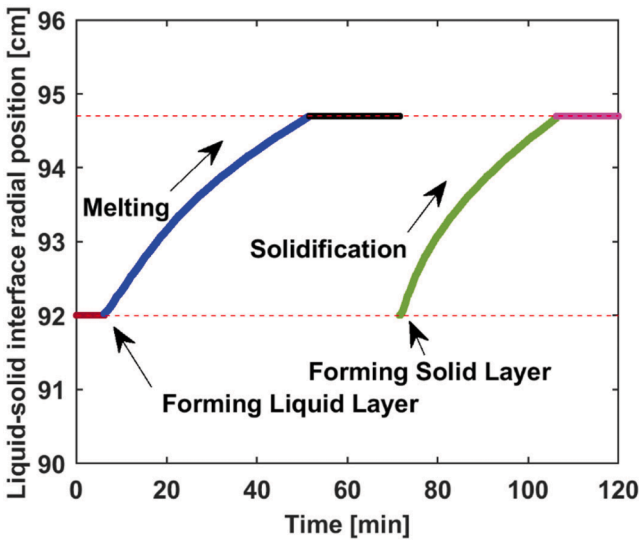

Fig. 10. PCM phase-change in HyTES (r = 0 is at the centre of the SA).

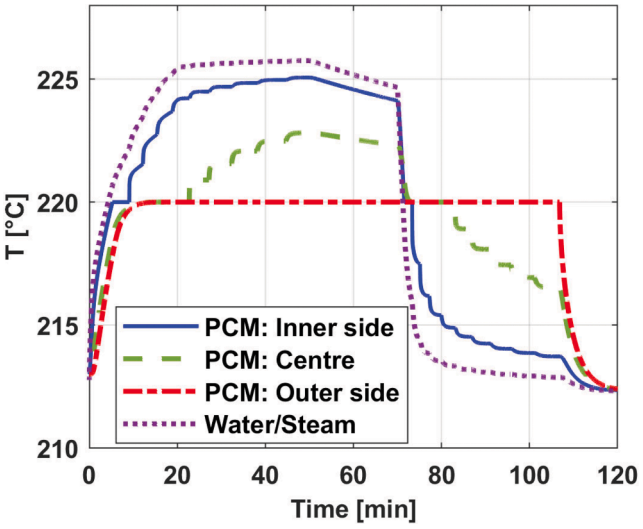

Fig. 11. Temperature of different compartments of HyTES.

process. Conversely, the temperature of the PCM located at a larger radial coordinate (i.e., PCM outer side) raises/decreases at a later stage during the charge/discharge process. The step-wise nature of the temperature profiles illustrated in Fig. 11 is due to the numerical discretisation along the radial direction employed to model the physical phenomena (see Fig. 9). Nonetheless, it is relevant to emphasise that the accuracy of such a modelling approach was proven to be adequate in Section 3.1.4 where model validation is reported.

4.1.3. Overall energy storage performance of the whole Hy-TES system under complete charge–discharge cycles

As in the case of any energy storage system, it is crucial to assess the behaviour of the total stored energy during the charge/discharge cycle. This is reported in Fig. 12, where contributions from each component of the HyTES subsystem are also illustrated. It is worthwhile to notice how the system allows different response-time for SA and PCM. While the former is a fast-responding energy storage, the latter instead provides a longer heat storage duration. The thermal energy capacity is investigated by comparing the results between HyTES and conventional SA under identical total volume.

The results in Fig. 12 clearly show how the proposed hybrid system,

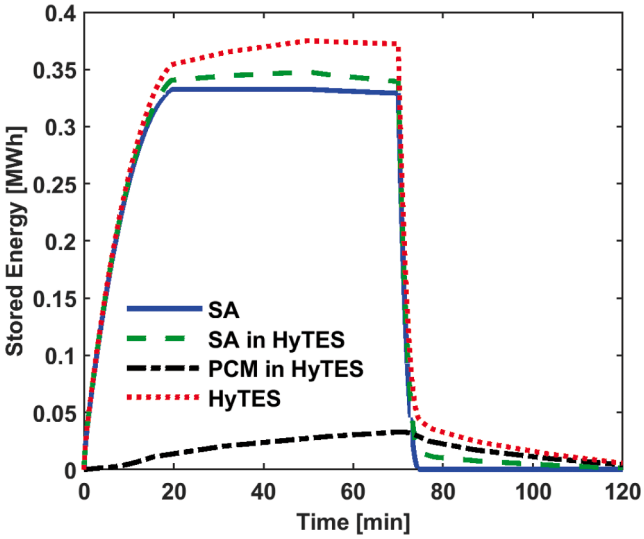

Fig. 12. State of charge of the HyTES.

compared to a conventional SA, provides a relevant 15 % increase in overall storage capacity with ~ 5 % of the volume dedicated to PCM. Such an increase in storage capacity is due to the multiple effects that the PCM subsystem has on the overall system behaviour. On its own PCM part store extra energy in the form of latent heat, as clearly shown in Fig. 13. In addition, the presence of the PCM stage allows the SA to indirectly accumulate more steam, leading to a further increase in the total amount of stored energy. This is caused by the exchange of heat that occurs between SA and PCM subsystems through the wall separating the two sections. According to the operation principle of SA, when fresh steam is introduced into the vessel, it cools down, and the existing water and steam are heated to a higher temperature, reaching a new equilibrium state. The heat absorbed by the PCM during the charging results in a delay in the system temperature rise. Hence, there is a lower temperature and saturation pressure in the HyTES. Due to the higher thermodynamic driving force, more steam is drawn into the vessel to eventually reach the pressure of the steam source. As the charging advances, more incoming steam is condensed in the HyTES (as is evident in Fig. 8b). A larger water mass indicates higher cumulative energy. Thus, that 15 % extra energy capacity arises from the superior performance of SA (5 %) in the HyTES and the PCM itself (10 %).

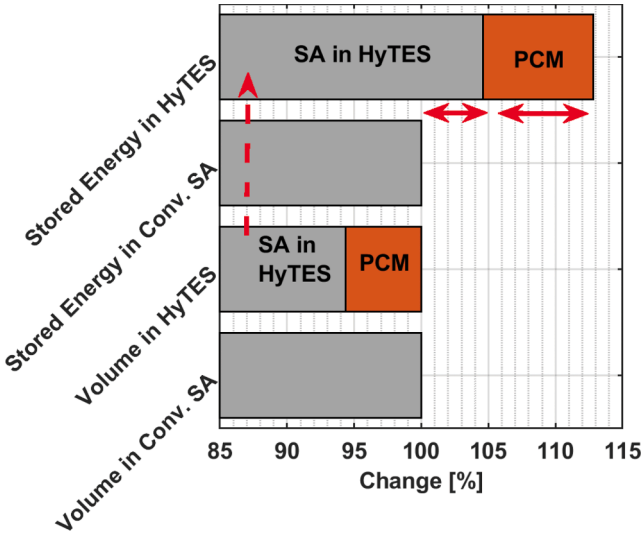

Fig. 13. HYTES capacity compared with conventional storage.

4.2. Technical parametric analysis

Although the key features characterising the dynamic behaviour of the HyTES system have been illustrated in the previous sections, it is also essential to understand how such behaviour is affected by the main technical parameters of HyTES systems. The ratio of HyTES energy storage capacity to the one of conventional SA was assessed for different amounts of PCM (i.e. volume) and PCM specific heat capacity (C_p) while the remaining parameters, including the radius of SA, are kept unchanged. In the cylindrical configuration, the relative amount of PCM is represented by a volumetric fraction and the ratio of total radius (R_2) to the radius of the base SA (R_1).

As a metric to show HyTES superiority over conventional SA for storing the heat, the energy capacity ratio is defined as the ratio of HyTES capacity to that of the base SA. The denominator of this ratio for all cases is the same, and the energy capacity ratio reveals the effect of hybridisation. As shown in Fig. 14, by adding PCM to the SA with a fixed configuration, the capacity can be increased up to 15 %, and the shaded region shows the best achievable performance. The optimum values found for the PCM to SA volume ratio is within 5 % to15%, where PCM's impact on capacity enhancement is more pronounced.

In order to clarify the rationale behind the initial increase and the subsequent decline in energy capacity ratio, the phase change profiles through the charging-discharging process are extracted for three configurations which are composed of identical SA and PCM with different thicknesses attached to it. The thickness of PCM in cases A, B and C are 20 mm, 40 mm, and 70 mm. The same number of elements and time-step are used; therefore, they can be compared. As shown in Fig. 15, the initial temperature of the PCM elements is below the melting point; therefore, the entire PCM is solid at the beginning of the HyTES operation. In the charging stage, the heat is transferred to the PCM, the melting is triggered from the inner element, and the neighbouring elements are also gradually involved. The ultimate position of the solid–liquid interface at the end of charging and idle stages depends on the heat flux, charging time, heat capacity, latent heat, and the melting point of the PCM. The contribution of the elements undergoing the phase change to store the heat is in the form of sensible heat and latent heat, while the contribution of the remaining ones is only in the form of sensible heat. As shown in Fig. 15, the interface in all cases is found almost at the same distance from the surface of SA, which means the amount of extra PCM embedded into the system does not play a significant role in the phase interface location. However, as shown in Fig. 14, it marginally alters the overall heat which can be stored by the HyTES. In case B, the solid elements perform as a heat sink, absorb sensible heat and postpone the melting of inner elements, which ultimately leads to an

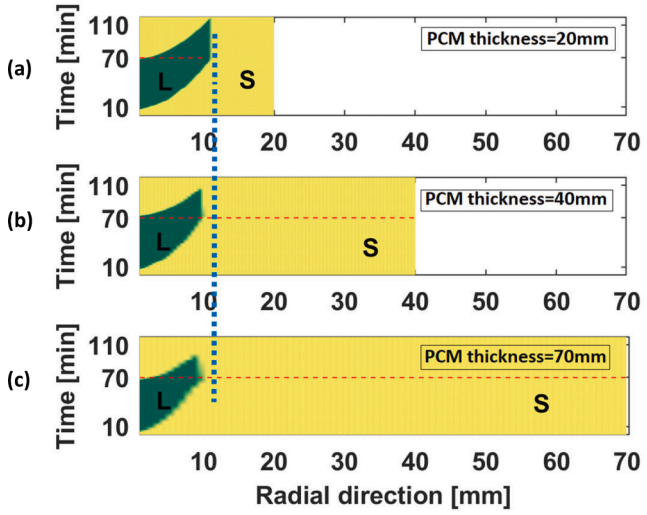

Fig. 15. Phase change profile in various PCM proportions (Red line: discharging time).

increase in the HyTES energy capacity. This sensible heat can be released during the discharging stage. However, when the amount of PCM exceeds 15 % (according to Fig. 14 and for case C in Fig. 15), it performs like an infinite heat sink. Although a large part of the PCM in case C is not involved in the phase change, the temperature is negligibly increased associated with the sensible heat; however, it is not enough to reach the melting temperature. This heat absorption also decelerates the melting of inner elements, and the liquid–solid interface is slightly displaced. In all cases, the effective thickness of PCM is found at about 11 mm. This limitation for the PCM amount also echoes the investigations by Dusek et al. [10], with a case study with a PCM thickness of 10 mm. Another investigation by Xu et al. [24] on PCM-based thermal energy storage for residential applications emphasises that exceeding the PCM thickness from 20 mm does not improve storage performance.

As shown in Fig. 14, the maximum energy capacity enhancement by hybridisation in a 2-hour timescale (shown in Fig. 6) is approximately 15 %, and according to the discussion above, this limit is not imposed by the amount of PCM. In the next step, the longer charging time than the base case, which was 50 min, is investigated. In order to fully take advantage of the PCM latent heat, the HyTES is simulated for a longer duration of charging, in which more PCM are involved in the phase change process. The enhancement of energy capacity of HyTES is compared in Fig. 16 for various latent heat values. The results confirmed

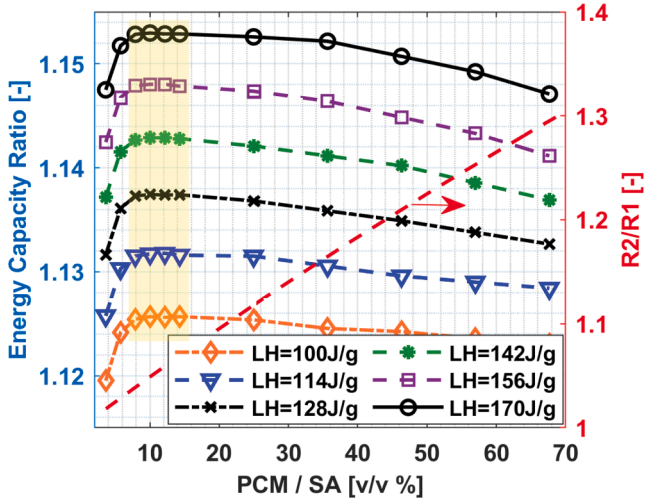

Fig. 14. Energy enhancement by various PCM proportions (fixed SA volume).

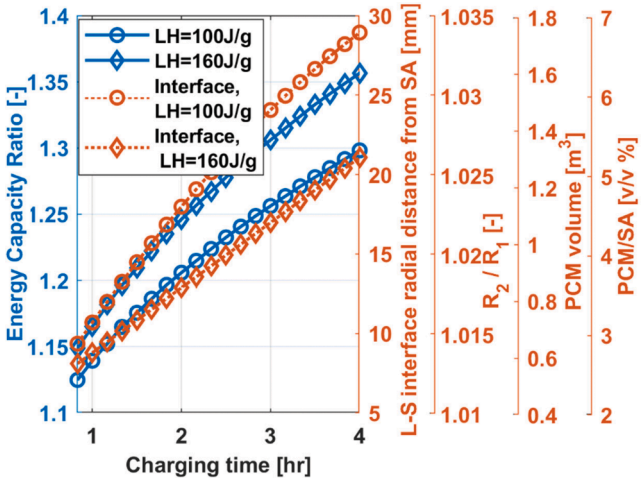

Fig. 16. Effect of charging time on the energy storage capacity ratio.

that a longer charging time for the same SA unlocks the hybridisation benefits, and the enhancement of the energy capacity can be up to 40 % for 4 h of charging, which is suitable for industrial applications. This value is consistent with 34 % additional stored energy in steam storage with phase change material casing reported by Dusek et al. [10]. However, it is only achievable with a longer charging time, which means an extended availability of the heat source. This figure also represents the liquid/solid interface displacement, in which the PCM with higher latent heat (circle marked dotted line) has a lower displacement. On the other hand, it has a higher energy capacity ratio, which stems from a higher heat transfer rate resulting from lower thermal resistance between the SA surface and the liquid–solid interface.

The effect of specific heat capacity on the energy capacity is also investigated and found to be insignificant for the present case study compared to the effect of latent heat. Fig. 17 shows the energy capacity ratio of HyTES for three different latent heat values and the associated marginal increase for using PCM with higher specific heat capacities. Fig. 17 shows that the latent heat has a dominant effect, while the average variation of HyTES capacity by altering the specific heat capacity is approximately 0.1 %, knowing that the specific heat capacity for the commercial PCMs with a melting point matching the operating temperature of steam accumulators (210 to 300 °C), for HyTES is lies within a narrow range of 1.5–1.57 $kJ/(kgK)$.

4.3. Economic evaluation

In this section, the findings of the economic investigation are presented. The industrial case study is a 3-hour steam demand in the food industry [19]. It is assumed that the system is operating continuously, and therefore, it is calculated that the system supplies 52GWh of thermal energy per year by providing low-pressure steam. The calculation is derived by scaling the 3-hour steam demand [19] to 360 days of operation.

The base line scenario consists of a boiler system sized to supply the maximum steam demand. Two alternative scenarios are comprised of a boiler coupled with an energy storage system, namely conventional SA or the HyTES system. Either the conventional SA or the HyTES can store surplus steam produced by the boiler at times of low demand for subsequent release to supplement the output of the boiler during time of high demand. In these two scenarios, the boiler generation capacity was considered to be lower than the maximum steam demand. In particular, four different boiler capacities were considered: 80 %, 65 %, 50 % and 37.5 % of the maximum capacity. Visually, each capacity is labelled with A, B, C and D in Fig. 18, which also shows the time evolution of the steam demand.

In scenarios A to D, either SA or HyTES supports the reduced-capacity boiler. The cooperation between the energy storage technology and boiler then allows the steam demand to be fully met. It is also extensively discussed by Çam et al. [26], who explored the plant economy by integrating thermal energy storage into the steam generation system. The author assessed up to 0.6 M€ additional profit, estimated as a 3.5 % increase in plant profit. The support of the energy storage technology would be in releasing steam during peak demand. In each case, when the instantaneous steam demand exceeds the boiler steam generation, the surplus steam demand is considered to be met by the energy storage technology (corresponding to the yellow highlighted area in Fig. 18). Conversely, when the demand is lower than the boiler generation capacity, the exceeding boiler generation capacity is used to charge the energy storage. The surplus steam demand and the deficit in boiler steam generation are reported in Fig. 19 for a range of relative boiler generation capacity, where 100 % capacity identifies the case where the boiler is sized to meet the maximum peak demand of steam. In particular, the time-averaged demands below and above the boiler capacity are balanced by using a boiler with 38 % lower capacity. This percentage echoes the ratio which is reported by SINTEF [27]. They found that the integration of the SA leads to covering the steam demand with a boiler capacity up to 41 % lower than the capacity of the current one.

In order to proceed further in the economic assessment, it is necessary to identify the capacity as well as the internal configuration of the HyTES system. Four cases with different steam supply configurations are defined for the economic assessment. In the base case, the energy is supplied by the gas boiler with a capacity adjusted to the maximum demand (according to Fig. 18). Alternatively, a conventional SA can support the gas boiler in peak shaving and valley filling in the steam supply. In addition, two HyTESs are assumed: one is designed for 50 min of charging, and the corresponding capacity ratio is approximately 1.15 (according to Fig. 14). The second HyTES is assumed for cases with a charging time of 4hrs that deliver a capacity ratio of 1.4 (as shown in Fig. 16). The potential amount of energy that each of those components can supply to meet the process demand within a four-hour time frame is shown in Fig. 20. This comparison is assessed based on two hybridisation approaches: a) Fixed volume (F) in which both HyTES and conventional SA have the same total volume in the comparison; b) retrofit design (R in which PCM layer can be added to the existing SA; therefore the overall volume increased. Moreover, what stands out in

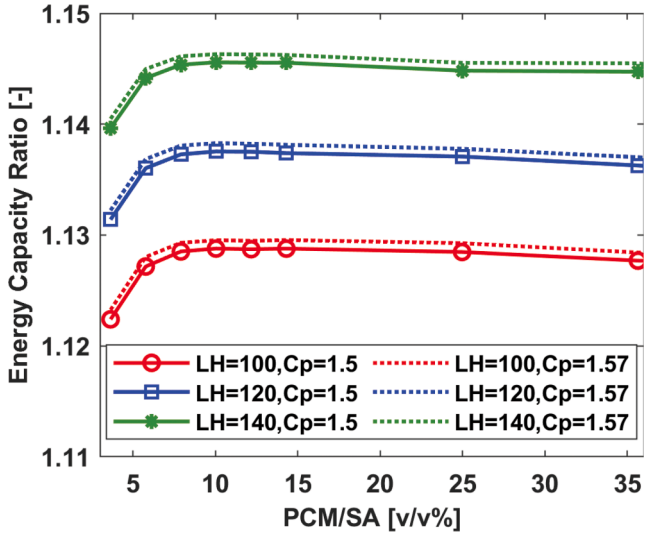

Fig. 17. Effect of amount of PCM, sensible heat and heat of the energy capacity ratio (Unit: LH [**kJ**/**kg**], Cp [**kJ**/(**kgK**)]).

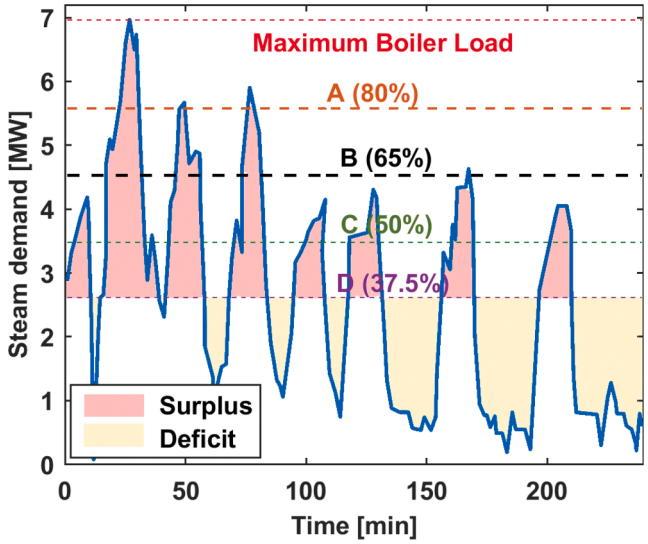

Fig. 18. PCM sub-model (Surplus and deficit zones for case D are highlighted).

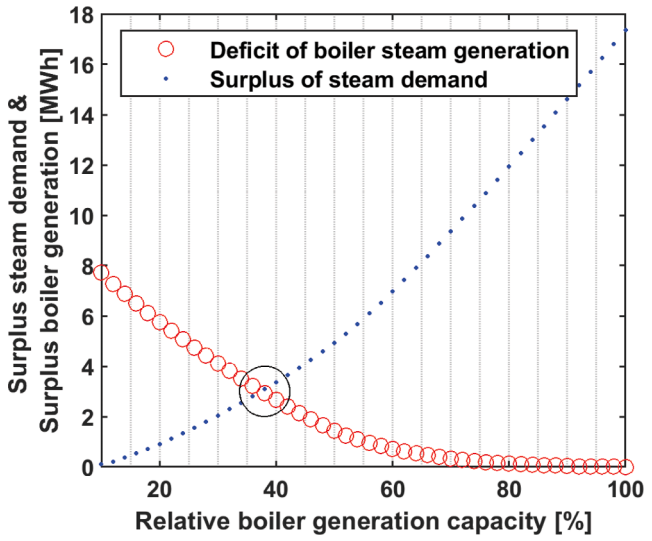

Fig. 19. Surplus steam demand and the surplus boiler generation capacity for various boiler capacities.

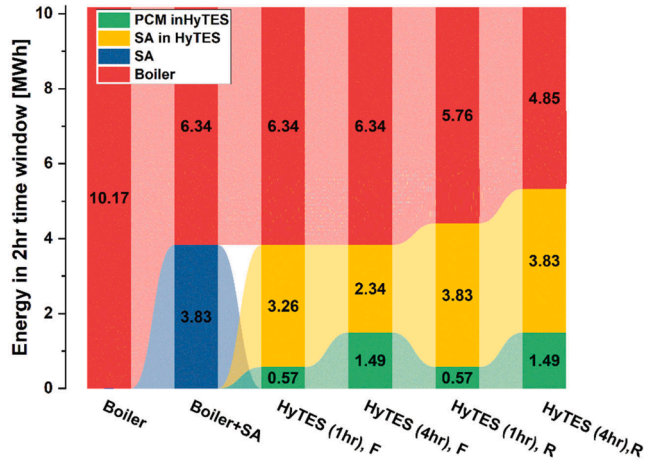

Fig. 20. Distribution of stored energy in different storage configurations for the food industry case study (R: retrofit, F: Fixed total volume).

this figure is the dominance of boiler duty in all cases, and the boiler is expected to operate steadily at this capacity, while axillary support from either SA or the HyTES operates only in peaks.

The CAPEX is calculated by the purchase equipment cost (PEC) of the boiler, which is a function of mass flow [2829], and the PEC of SA, which is taken from a European commercial price list [30] verified by literature data [3113]. A 2-year (2021–22) average EUR/USD exchange rate of 1.162 is used for non-European price data [32]. The results are illustrated in Fig. 21a for SA and Fig. 21b for boiler, in which the data are updated for the year 2021 by Chemical Engineering Plant Cost Index (CEPCI) index (see Fig. 22).

The costs associated with the steam supply unit can be assessed as generation cost (GC), accounting for the annual fuel costs (FC) and annual non-fuel operating cost (O&M), as well as the capital cost (CAPEX).

$$GC = CAPEX + TL(O\&M_{non-fuel} + O\&M_{fuel}) \quad (11)$$

where TL is the technology lifetime, which is commonly 25 years for the boiler systems.

According to the literature which is listed in Table 2, the average unit price is estimated as 20 €/kWh to 140 €/kWh for the SA and within 10€/kWh to 50 €/kWh for the PCM. Moreover, O&M costs are estimated as a percentage of the CAPEX. The annual O&M cost is within 4 % to 21 % of the CAPEX, while the fuel cost (FC) highly depends on the gas price,

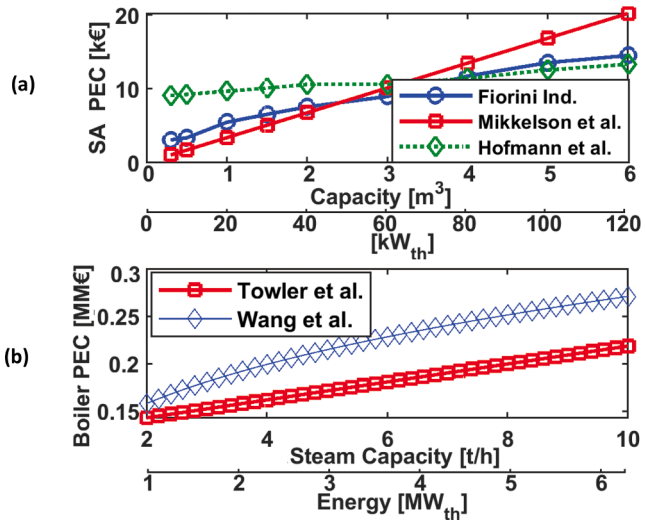

Fig. 21. Cost curves for SA and the gas boiler.

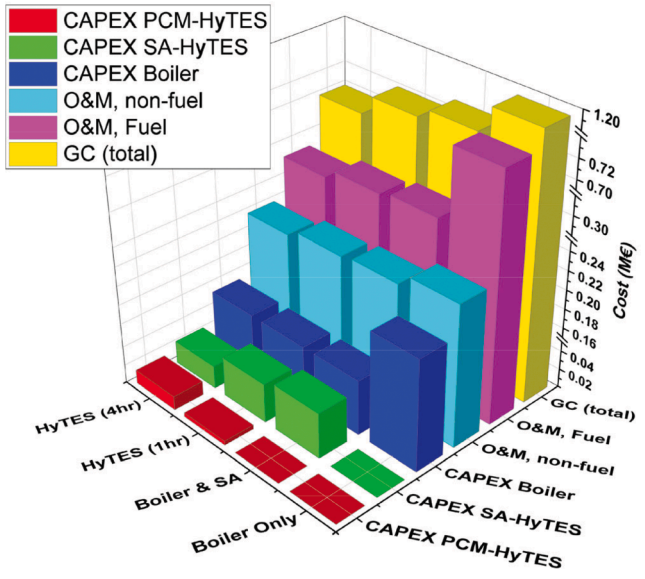

Fig. 22. Generation cost (GC) and CAPEX components for various scenarios.

Table 2
Cost calculation assumptions.

Parameter	Range	selected value	Ref.
SA specific price [€/kWh]	[20–140]	40	[333431353637]
PCM specific price [€/kWh]	[10–50]	30	[3839]
$\frac{\text{Boiler O\&M cost}}{\text{CAPEX}}$ [%]	[4–21]	4.5	[34,40,41,42,43,44]
average gas price (EU) [c€/kWh]	–	2.79	[45 46]
Natural gas net calorific value (NCV) [MJ/m^3]	[34.2–37.2]	35.3	[47]
Boiler steam/energy [(kg/h)/kW]Ratings (F&A 100° C)	–	0.63	–
Gas boiler Lifetime [yr]	–	25	[34]
TES Lifetime [yr]	[25–40]	25	[34]

roughly 20 % to 40 % of the CAPEX. However, the fuel cost is estimated based on 7500 yearly operating hours and the 2-year EU-average gas price for non-household consumers, which was 0.0279 €/kWh in 2020–2022.

The generation cost is assessed for all cases and compared with the base design in which the boiler fulfils the total steam demand, which is shown in **Error! Reference source not found.**. Although the fuel cost dominates the GC, the CAPEX components are remarkably different between the boiler only and the alternative configurations. The financial impact on the end-user is assessed by the estimation of the generation cost of the plant lifetime. The saving in capital cost is calculated as 5.2 %, and GC is notably reduced by 38 % when SA is deployed. When using the HyTES, a 5 % decrease in the CAPEX is found compared to the conventional SA. However, this reduction is mainly mirrored by the CAPEX, which is also a part of GC when HyTES is deployed. Furthermore, the O&M cost saving is estimated at 16.5 % and 21 % for SA and HyTES.

5. Conclusions

This paper aimed at comprehensively assessing the technical and economic viability of hybrid thermal energy storage (HyTES) to replace conventional steam accumulators (SA) for industrial applications. The study thoroughly addressed the hybridisation concept, principle of operation, limiting factors affecting the performance of HyTES, short-term and long-term financial benefits. The main conclusions are summarised as follows:

- HyTES is composed of conventional SA and high-temperature PCM layers on the surface of the SA. The energy capacity of HyTES in storing the surplus steam and releasing energy during the peak depends on the charging time, PCM thermal property, and the amount of PCM embedded in the SA. The extra energy capacity of HyTES arises from incorporating the PCM, which stores a considerable amount of heat on its own as well as supports the SA in receiving additional steam. On the other hand, due to the slow response of PCM in charging and discharging, the overall duration of HyTES response would be longer than that of the conventional SA.
- The extra heat capacity of HyTES appears to be dominated by latent heat energy; therefore, the part of the PCM which reaches the melting point and is involved in phase change has a key role in the energy capacity enhancement. Although the remaining parts of the PCM store the heat in the form of sensible heat, the contribution to the overall extra heat capacity is less than 1 %. However, those parts can be effectively involved for a longer charging time. The energy capacity enhancement of HyTES is shown ranging from 15 % to 45 %, which are estimated for charging time from 1 to 4 h. Indeed, utilising PCM with higher latent heat can further improve the capacity of HyTES.
- Although the upper bound of additional storage of HyTES is found as 45 %, it is only achievable when the heat source for charging is available for about 4 h. In retrofitting the existing SA, the predetermined process condition, particularly steam source and sink caps the energy storage enhancement.
- The economic analysis was carried out by estimating investment and O&M costs. The use of HyTES noticeably reduces both the investment and O&M costs, which ultimately affects the long-term steam generation cost. The CAPEX of a system with HyTES is found to be 5 % less than the case with conventional SA. HyTES improves industrial plant economics by reducing generation cost, which includes the CAPEX and O&M cost.

In conclusion, it was demonstrated how HyTES outperformed conventional SA to shave the steam peaks. By the presented discussion regarding the cost impact and efficiency improvement, the HyTES has more chance of being accepted by industry. However, the magnitude of enhancement depends on the industrial process and the type of intermittency in steam demand. HyTES offers higher capacity and longer duration of storage with financial benefits in the short and long terms. In this sense, the results presented in this work provide an understanding of the feasibility of HyTES in industries. However, HyTES has the potential to be further adapted to industrial processes and contribute to improved flexibility beyond the potential already demonstrated in this paper.

Future works

The present study is confined to thermal analysis and economic assessment with a more technically conceptual approach. The economic part is based on the average-size SA for a representative industrial unit from the food sector. However, the result is mainly discussed using dimensionless ratios and relative changes to state the performance of the equipment. Future works could expand the current work by extending the potential of SA in plants with various scales in different sectors. The present economic assessment is based on average price indexes for SA and PCM for CAPEX calculations. The unit prices are associated with order quantity, type and supplier. Also, SA price highly depends on the steel price. Also, the current assessment is conducted based on natural gas boilers, and the fuel cost margin is neglected for the operating cost. Alternative fuels with corresponding margins could be considered in further studies. However, these assumptions reduce the complexity of economic assessment to clearly gauge the profitability of HyTES technology. Future works can also address the environmental impacts linked with energy resources. This part can be assessed in the form of an LCA analysis of HyTES, using the same approach of representative environmental studies for thermal energy storage systems [1448]. It will determine the environmental sustainability of HyTES configuration from a full life cycle perspective.

CRediT authorship contribution statement

Pouriya H Niknam: Conceptualization, Methodology, Software, Validation, Formal analysis, Investigation, Writing – original draft, Visualization. **Adriano Sciacovelli:** Conceptualization, Methodology, Validation, Investigation, Writing – review & editing, Supervision, Resources, Project administration, Funding acquisition.

Declaration of Competing Interest

The authors declare that they have no known competing financial interests or personal relationships that could have appeared to influence the work reported in this paper.

Data availability

Data will be made available on request.

Acknowledgments

This work was supported by the European Union's Horizon 2020 research and innovation programme (SO WHAT Project; grant number 847097).

References

[1] HM Government. Net Zero Strategy: Build Back Greener; 2021. Accessed: Feb. 25, 2022. [Online]. Available: https://assets.publishing.service.gov.uk/government/uploads/system/uploads/attachment_data/file/1033990/net-zero-strategy-beis.pdf.
[2] WSP and Parsons Brinckerhof. Industrial Decarbonisation & Energy Efficiency Roadmaps to 2050; Apr. 2015. Accessed: Feb. 25, 2022. [Online]. Available: https://assets.publishing.service.gov.uk/government/uploads/system/uploads/attachment_data/file/416676/Ceramic_Report.pdf.
[3] Committee on Climate Change. "Net Zero The UK's contribution to stopping global warming, London, May 2019. Accessed: Feb. 25, 2022. [Online]. Available: https://www.theccc.org.uk/wp-content/uploads/2019/05/Net-Zero-The-UKs-contribution-to-stopping-global-warming.pdf.

[4] Haider M, Werner A. "An overview of state of the art and research in the fields of sensible, latent and thermo-chemical thermal energy storage", e iEin Überblick zum Stand der Technik und Forschung im Bereich sensibler, latenter und thermochemischer Wärmespeicherung. Elektrotechnik und Informationstechnik 2013;130(6):153–60.

[5] Zhang H, Baeyens J, Cáceres G, Degrève J, Lv Y. Thermal energy storage: Recent developments and practical aspects. Prog Energy Combust Sci 2016;53:1–40.

[6] Kuznik F, Opel O, Osterland T, Ruck WKL. Thermal energy storage for space heating and domestic hot water in individual residential buildings. In: Advances in Thermal Energy Storage Systems Advances in Thermal Energy Storage Systems. Elsevier; 2021. p. 567–94.

[7] Ding Z, Wu W, Leung M. Advanced/hybrid thermal energy storage technology: material, cycle, system and perspective. Renew Sustain Energy Rev 2021;145:111088.

[8] Zauner C, Hengstberger F, Mörzinger B, Hofmann R, Walter H. Experimental characterization and simulation of a hybrid sensible-latent heat storage. Appl Energy 2017;189:506–19.

[9] Dusek S, Hofmann R. Modeling of a hybrid steam storage and validation with an industrial ruths steam storage line. Energies 2019;12(6):1–21. https://doi.org/10.3390/en12061014.

[10] Dusek S, Hofmann R, Gruber S. Design analysis of a hybrid storage concept combining Ruths steam storage and latent thermal energy storage. Appl Energy 2019;251:113364.

[11] Pernsteiner D, Kasper L, Schirrer A, Hofmann R, Jakubek S. Co-simulation methodology of a hybrid latent-heat thermal energy storage unit. Appl Therm Eng 2020;178:115495. https://doi.org/10.1016/j.applthermaleng.2020.115495.

[12] Kasper L, Pernsteiner D, Koller M, Schirrer A, Jakubek S, Hofmann R. Numerical studies on the influence of natural convection under inclination on optimal aluminium proportions and fin spacings in a rectangular aluminium finned latent-heat thermal energy storage. Appl Therm Eng 2021;190:116448.

[13] Hofmann R, Dusek S, Gruber S, Drexler-Schmid G. Design optimization of a hybrid steam-PCM thermal energy storage for industrial applications. Energies 2019;12(5):1–25. https://doi.org/10.3390/en12050898.

[14] Venettacci S, Cozzolino R, Ponticelli GS, Guarino S. Environmental and economic life cycle assessment of thermal energy storage based on organic phase change material embedded in open-cell copper foams. Sustain Prod Consum 2022;29:387–405. https://doi.org/10.1016/j.spc.2021.10.026.

[15] Lund HF. operating costs and procedures. J Air Pollut Control Assoc 1969;19(5):315–21.

[16] EIA. Levelized Costs of New Generation Resources in the Annual Energy Outlook 2021; 2021.

[17] Walker ME, Lv Z, Masanet E. Industrial steam systems and the energy-water nexus. Environ Sci Technol 2013;47(22):13060–7. https://doi.org/10.1021/es403715z.

[18] Dusek S, Hofmann R. A hybrid energy storage concept for future application in industrial processes. Therm Sci 2018;22(5):2235–42. https://doi.org/10.2298/TSCI171230270D.

[19] Hechelmann R-H, Seevers J-P, Otte A, Sponer J, Stark M. Renewable energy integration for steam supply of industrial processes—a food processing case study. Energies 2020;13(10):2532. https://doi.org/10.3390/en13102532.

[20] Stevanovic VD, Maslovaric B, Prica S. Dynamics of steam accumulation. Appl Therm Eng 2012;37:73–9. https://doi.org/10.1016/j.applthermaleng.2012.01.007.

[21] Mohammed HI, Talebizadehsardari P, Mahdi JM, Arshad A, Sciacovelli A, Giddings D. Improved melting of latent heat storage via porous medium and uniform Joule heat generation. J Energy Storage 2020;31:101747. https://doi.org/10.1016/j.est.2020.101747.

[22] PCMproducts. PlusICE Range - pcm products," 2021. https://www.pcmproducts.net/files/PlusICE Range 2021-1.pdf.

[23] Humbert G, Roosendaal C, Swanepoel JK, Navarro HM, Le Roux WG, Sciacovelli A. Development of a latent heat thermal energy storage unit for the exhaust of a recuperated solar-dish Brayton cycle. Appl Therm Eng 2022;216:118994. https://doi.org/10.1016/j.applthermaleng.2022.118994.

[24] Stevanovic VD, Petrovic MM, Milivojevic S, Maslovaric B. Prediction and control of steam accumulation. Heat Transf Eng 2015;36(5):498–510. https://doi.org/10.1080/01457632.2014.935226.

[25] Al Siyabi I, Khanna S, Mallick T, Sundaram S. An experimental and numerical study on the effect of inclination angle of phase change materials thermal energy storage system. J Energy Storage 2019;23:57–68. https://doi.org/10.1016/j.est.2019.03.010.

[26] Çam E. Optimal dispatch of a coal-fired power plant with integrated thermal energy storage [Online]. Available: Cologne 2020. http://hdl.handle.net/10419/227509.

[27] SINTEF. Cycles RA3, Fossil-free steam production for Nidar Orkla," 2021. https://www.sintef.no/projectweb/higheff/results/cycles-ra3/ (accessed Aug. 31, 2022).

[28] Towler G, Sinnott R. Chemical Engineering Design: SI Edition (Chemical Engineering Series). 6th ed. Butterworth-Heinemann; 2019.

[29] Wang L, Yang Y, Dong C, Morosuk T, Tsatsaronis G. Parametric optimization of supercritical coal-fired power plants by MINLP and differential evolution. Energy Convers Manag 2014;85:828–38. https://doi.org/10.1016/j.enconman.2014.01.006.

[30] Fiorini industries. Fiorini industries catalogue – Price List 2016. *http://nemomont.com/wp-content/uploads/2016/10/FIORINI-CATALOGUE-AND-PRICE-2016-826080052.pdf*.

[31] Mikkelson D, Frick K, Bragg-Sitton S, Doster JM. Phenomenon identification and ranking table development for future application figure-of-merit studies on thermal energy storage integrations with light water reactors. Nucl Technol 2022;208(3):437–54. https://doi.org/10.1080/00295450.2021.1906473.

[32] ECB. Euro Foreign Exchange Reference Rates since 1999. European Central Bank Statistics, 2016. https://www.ecb.europa.eu/stats/exchange/eurofxref/html/index.en.html (accessed Sep. 20, 2022).

[33] Buseth ER. Renewable Energy in Longyearbyen. NTNU, 2020. [Online]. Available: https://ntnuopen.ntnu.no/ntnu-xmlui/handle/11250/2778263.

[34] Chikri YA. Hybrid boiler systems in the Dutch industry. Delft University of Technology. [Online]. Available: https://repository.tudelft.nl/islandora/object/uuid%3A138874fa-32d2-4319-80fa-c089c3feef72.

[35] Kauko H, Sevault A, Og AB, Drexler-Schmid G. Thermal storage for improved utilization of renewable energy in steam production. 2019. [Online]. Available: https://app.cristin.no/results/show.jsf?id=1744103.

[36] Gibb D et al. Applications of Thermal Energy Storage in the Energy Transition – Benchmarks and Developments." [Online]. Available: https://www.sintef.no/en/publications/publication/1646046/.

[37] Consortium M. MAGNITUDE D1.2 -Technology and case studies factsheets," 2019. [Online]. Available: https://www.magnitude-project.eu/wp-content/uploads/2019/07/MAGNITUDE_D1.2_EIFER_Final_Submitted.pdf.

[38] Radcliffe J, Li Y. Thermal energy storage in Scotland; 2015. [Online]. Available: https://www.climatexchange.org.uk/media/1393/thermal_energy_storage_in_scotland.pdf.

[39] Hauer A. Storage Technology Issues and Opportunities," CERT Energy Storage Workshop, Paris; 2011. [Online]. Available: https://iea.blob.core.windows.net/assets/imports/events/337/Hauer.pdf.

[40] Yeh S, Rubin ES. A centurial history of technological change and learning curves for pulverized coal-fired utility boilers. Energy 2007;32(10):1996–2005. https://doi.org/10.1016/j.energy.2007.03.004.

[41] Fleiter T, Steinbach J, Ragwitz M. Mapping and analyses of the current and future (2020 - 2030) heating/cooling fuel deployment (fossil/renewables)," 2016. [Online]. Available: https://ec.europa.eu/energy/sites/ener/files/documents/mapping-hc-final_report-wp2.pdf.

[42] BELTRAN H. MODERN PORTFOLIO THEORY APPLIED TO ELECTRICITY GENERATION PLANNING. University of Illinois at Urbana-Champaign; 2008. [Online]. Available: https://core.ac.uk/reader/4821190.

[43] Capital Cost and Performance Characteristic Estimates for Utility Scale Electric Power Generating Technologies. Washington, DC 20585, 2020. [Online]. Available: https://www.eia.gov/analysis/studies/powerplants/capitalcost/.

[44] Lyons S. Industrial Fuel Switching Market Engagement Study. Cambridge CB5 8AQ.

[45] Eurostat. Natural gas price statistics; 2022. https://ec.europa.eu/eurostat/statistics-explained/index.php?title=Natural_gas_price_statistics.

[46] "Gas prices for non-household consumers - bi-annual data (from 2007 onwards)," Eurostat, 2022. https://appsso.eurostat.ec.europa.eu/nui/show.do?dataset=nrg_pc_203&lang=en (accessed Aug. 31, 2022).

[47] IAE. Key World Energy Statistics 2021; 2021. [Online]. Available: https://www.iea.org/reports/key-world-energy-statistics-2021.

[48] Chocontá Bernal D, Muñoz E, Manente G, Sciacovelli A, Ameli H, Gallego-Schmid A. Environmental assessment of latent heat thermal energy storage technology system with phase change material for domestic heating applications. Sustainability 13(20):11265. 2021, doi: 10.3390/su132011265.